Absorption Tails and Extinction in Luminescent Solar Concentrators

Alan A. Earp, Jim B. Franklin and Geoff B. Smith*

Department of Physics and Advanced Materials, University of Technology Sydney, PO Box 123 Broadway, NSW 2007, Australia

**Corresponding author: alan.earp@uts.edu.au*

Abstract

Non-UV photoexposure of luminescent solar concentrators (LSC's) can produce photoproducts which causing additional extinction at wavelengths somewhat longer than the main dye absorption peak. This is extremely deleterious to luminous output in collectors of useful lengths. An experimental method that enables the subdivision of tails extinction in an LSC into absorbed and scattered components is described. The relevant theory is outlined, and experimental results are presented for a PMMA LSC containing *Lumogen F083* dye. For this sample, tails absorption increased significantly with outdoor exposure, while tails scattering remained constant. Further measurements indicate that LSC luminous output is around five times more sensitive to tails absorption than to fluorescence quenching.

OCIS Codes:

300.6280, 290.2200, 290.5820, 260.2510

1. Introduction

Luminescent Solar Concentrators (LSCs) have been widely studied in the past 30 years for their potential in collecting and concentrating solar energy. LSCs consist of a matrix with high optical clarity (such as PMMA, glass or sol-gel), doped with a fluorescent species (such as a dye or quantum

dots) that absorbs both direct and diffuse solar radiation, and isotropically emits light at longer wavelengths. A large fraction of the emitted light is trapped by total internal reflection and concentrated towards the edges of the collector. This concentrated edge-light is predominantly used for photovoltaic electricity generation [1-6], although it has also been used for heat generation [7] and lighting [8].

One of the most significant remaining technical obstacles preventing widespread utilisation of LSCs is the limited photostability of the fluorescent species [4, 9-11]. Photodegradation of LSC's leads to reduced LSC efficiency due to two main processes:

1. **Fluorescence quenching** – photoexcited dye molecules gradually break down due to interactions with impurities in the matrix or with UV radiation if present, resulting in reduced absorption and fluorescence intensities with exposure.
2. **The formation of photoproducts –** photodegradation can lead to the formation of by-products, causing increased 'tails' extinction at longer wavelengths than the main dye absorption edge[7, 12].

From earlier work on LSC's it is evident that very low levels of extinction in the 'tails region' (at longer wavelengths than the main dye absorption peak) can lead to significant reductions in luminous output [8, 13]. Hence monitoring the tails absorption is an important exercise that can highlight significant sources of loss in exposed LSC's.

This article focuses on the analysis of extinction caused by photoproducts. If photoproducts form in an LSC during exposure, an important step in the remedial process is to identify the light loss mechanism. Depending on the nature of the dye degradation mechanism, photoproducts may cause extinction losses either by increased non-fluorescing absorption or by increased scattering. Matrix scattering losses in an LSC can be experimentally measured [14], as can total extinction losses via

measurements of transmission along the LSC long axis [7]. However, experimental measurements of absorption and scattering generally require two different sets of equipment and different sized samples. The advantage of the experimental method presented below is that it enables the subdivision of light travelling longitudinally inside an LSC into transmitted, absorbed and scattered components, using the same LSC sample with a single set of equipment. This analysis technique enables the identification of the primary light loss mechanism in an exposed LSC, which can help determine the particular degradation mechanism at work. The theory and some example experimental results are presented below.

2. Experimental Method and Theory

2.1 Sample Preparation

For this study, LSC's were produced from 2 mm thick cast PMMA sheets containing *Lumogen F083* fluorescent dye (BASF) at a concentration of 120 ppm, obtained from a commercial supplier. This green dye has absorption and emission maxima at 472 nm and 518 nm respectively. A clear reference sheet was also provided, produced with exactly the same process and ingredients, but omitting the dye. Clear and dyed LSC samples with dimensions 1200 mm x 150 mm x 2 mm were produced by cutting sections from the master sheets and diamond polishing the four thin edges with a *C.R. Clarke 1550* diamond polisher.

2.2 Test Equipment

To experimentally isolate the extinction losses due to scattering and absorption, the following equipment was used. As schematically represented in Figure 1, LSC samples of length *L* were illuminated with an optic fibre illuminator (*Encore*^{TM} by *Lumenyte)* containing a 150W metal halide lamp, connected to a 1 m long, 18 mm diameter polymer optic fibre (*Lumenyte*) and a 1 mm x 20 mm slit. Output spectra were measured with a fibre optic integrating sphere (*FOIS-1, Ocean*

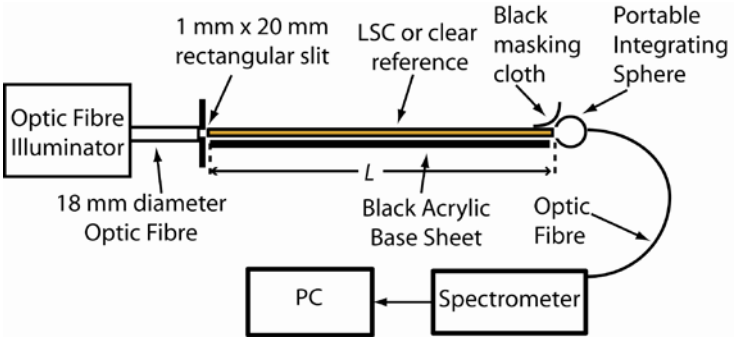

Figure 1 (Color online) Experimental setup for transmission measurements

Optics), consisting of a 38 mm diameter integrating sphere with a 9.5 mm diameter sample port, connected via a 50 μm diameter optic fibre to a *USB2000* UV-Visible spectrometer (*Ocean Optics*). Spectra were recorded with a PC using *Spectrasuite*^{TM} software (*Ocean Optics)*. Stray light was excluded from the measurement by placing a black cloth over the top surface of the LSC adjacent to the integrating sphere port, and by using a black acrylic base sheet.

2.3 Transmission Measurements

The tails transmission of the LSC was measured as follows. Initially, the light source was coupled into the clear reference sheet, and the output signal at its end surface, $E_C(\lambda)$, was measured with a portable integrating sphere and a spectrometer according to the setup shown in Figure 1. The spectral power entering the sample is not easily measured directly due to geometrical coupling losses at the entry surface. Hence the spectral power immediately inside the clear reference entry surface, $P_o(\lambda)$, was calculated from the output signal as follows:

$$P_o(\lambda) = E_C(\lambda)\, w_C / [w_{\text{det}} \tau (1 - f)\, \Delta\lambda] \qquad \text{(counts.sec}^{-1}\text{.nm}^{-1}\text{)} \qquad (1)$$

Where

$E_C(\lambda)$ = measured spectrometer signal from clear reference sheet (counts)
w_C = width of clear reference sheet (m)
w_{det} = width of detector port on integrating sphere (m)
τ = spectrometer integration time (seconds); A value of 50 msec was used for the transmission measurements
$\Delta\lambda$ = wavelength interval (nm)

f = matrix loss factor; the fraction of the light source lost in the clear reference sheet due to matrix extinction and Fresnel reflection at the far end;

The matrix loss factor f was calculated as follows:

$$f = R_{end} + 1 - \exp(L\alpha_m) \quad (2)$$

Where

R_{end} = Fresnel reflection loss at the far end surface of the LSC (for this study, $n_{PMMA} = 1.5$ and $n_{air}=1$, so $R_{end} = 0.04$),

L = length of clear reference (m)

α_m = extinction coefficient of clear matrix (measured with a monochromatic laser).

For the LSC sample in this study, a representative value of $\alpha_m = 0.098$ m^{-1} was measured with a green laser at $\lambda = 532$ nm, which is near the two primary emission peak wavelengths of *Lumogen F083* (492 nm and 516 nm). Calculation of equation (2) for a 1.2 m long LSC yielded a matrix loss factor of $f = 0.151$ for the clear reference sample.

The light source was then coupled into the dyed LSC using the same setup shown in Figure 1, and the output signal from its end surface, $E_D(\lambda)$, was recorded. The spectral power transmitted by the LSC, $P_T(\lambda)$, was calculated as follows:

$$P_T(\lambda) = E_D(\lambda)\, w_D / [w_{\det}\tau(1 - R_{end})\Delta\lambda] \text{ (counts.sec}^{-1}\text{.nm}^{-1}\text{)} \quad (3)$$

Where

$E_D(\lambda)$ = measured spectrometer signal at the far end of the dyed LSC (counts)

w_D = width of dyed LSC (m)

R_{end} = Fresnel reflection losses at end surface of LSC ($R_{end} = 0.04$)

Unlike equation (1), the correction factor in brackets in equation (3) does not include intrinsic matrix losses, so that the LSC matrix losses are included in the transmission measurement. The transmission spectrum of the LSC, $T(\lambda)$, was calculated by dividing the transmitted spectral power $P_T(\lambda)$ by the input spectral power $P_o(\lambda)$:

$$T(\lambda) = P_T(\lambda) / P_o(\lambda) \quad (4)$$

The mean tails transmission, $\overline{T}$, was calculated by averaging $T(\lambda)$ over the tails wavelength region for the particular dye. For the Lumogen F083 dye used in this study, the tails region is 550 nm $\leq \lambda \leq$ 750 nm. However, for this study, calculations were made over the wavelength range 600 nm $\leq \lambda \leq$ 750 nm, due to excess emission below 600 nm (as described below).

2.4 Scattering Measurements

One of the advantages of the experimental method presented in this article is that the same equipment can be used to measure both the tails transmission and the scattering intensity from the side of the LSC. As illustrated in Figure 2, the scattering intensity $E_x(\lambda)$ was recorded at a fixed lateral distance, *x*, from the LSC entry surface, with the integrating sphere positioned at the side of the LSC. $E_x(\lambda)$ was measured at *N* different positions, spaced evenly along the side of the LSC, with an integration time of 1.2 seconds. For this study, the collector length was *L* = 1.2 m, and $E_x(\lambda)$ was measured at 10 cm intervals between *x* = 0.1 m and *x* = 1.1 m (*N = 11)*. To ensure that the scattering measurements only contain light travelling in the forward direction, back-reflected light from the LSC end surface was excluded by placing black absorbing tape across the entire width of the LSC, on the top surface near the output end.

The total spectral power scattered from the top, bottom and sides of the sheet, $P_s(\lambda)$, was calculated by summing the measured values of $E_x(\lambda)$ over all *x* positions, and multiplying by four.

$$P_S(\lambda) = 4\sum_{x_1}^{x_N} E_x(\lambda)dx/\left(w_{\det}\tau\right)\Delta\lambda \qquad \text{(counts.sec}^{-1}\text{.nm}^{-1}\text{)} \qquad (5)$$

Where

$E_x(\lambda)$ = spectral intensity at the LSC side surface, *x* cm from its entry surface (counts)
τ = Spectrometer integration time used for measurement of $E_x(\lambda)$ (sec)
dx = LSC length interval represented by each measurement (m)

The sum was multiplied by four, assuming isotropic scattering leading to equal scattered intensities from the top, bottom, left and right hand sides of the LSC. The scattering spectrum, $S(\lambda)$ was calculated by dividing the scattered spectral power $P_S(\lambda)$ by the input spectral power $P_o(\lambda)$:

$$S(\lambda) = P_S(\lambda)/P_o(\lambda) \qquad (6)$$

The mean scattered fraction, $\overline{S}$, was calculated by averaging $S(\lambda)$ over the effective tails region of the dye.

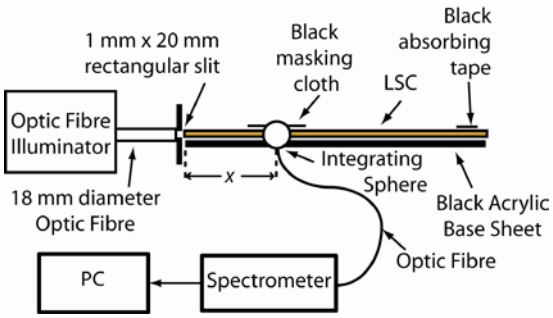

Figure 2 (Color online) Experimental setup for scattering measurements

2.5 Absorption

After measuring the transmission and scattering spectra, calculation of the absorption spectrum, *A(λ)*, was straightforward. Photons travelling lengthwise through an LSC must be either transmitted, scattered or absorbed. Therefore, to uphold the conservation of energy principle, the three components must sum to unity at each wavelength.

$$T(\lambda) + S(\lambda) + A(\lambda) = 1 \tag{7}$$

When properly dissolved, most suitable dyes for LSC's have negligible absorption in the tails region, so any significant tails absorption is due to photoproducts or impurities. However, this equation does not hold for wavelengths where dye emission is present, as some photons at these wavelengths have been converted by fluorescence from lower wavelength photons. Hence for this type of analysis, the tails region should be chosen such that dye emission is excluded. It follows from equation (7) that the mean values of the three components must also sum to unity.

$$\overline{T} + \overline{S} + \overline{A} = 1 \tag{8}$$

Therefore, the absorption spectrum, *A(λ)*, and the mean tails absorption $\overline{A}$ are calculated by substitution of the measured tails transmission and scattering values into equations (7) and (8) respectively.

3. Results and Discussion

3.1 Tails Extinction

Experimental results are presented below for the green LSC described in section 2.1. The LSC was initially tested before exposure, then again after six days' exposure to sunlight underneath a UV cover, which blocks all UV radiation below 340 nm. The measured spectra are presented in Figure 3, and in the region from 500 nm $\leq \lambda \leq$ 600 nm, the measured scattering component contains excess signal above a Rayleigh scattering curve fitted to the data (dotted line). Moreover, the additional

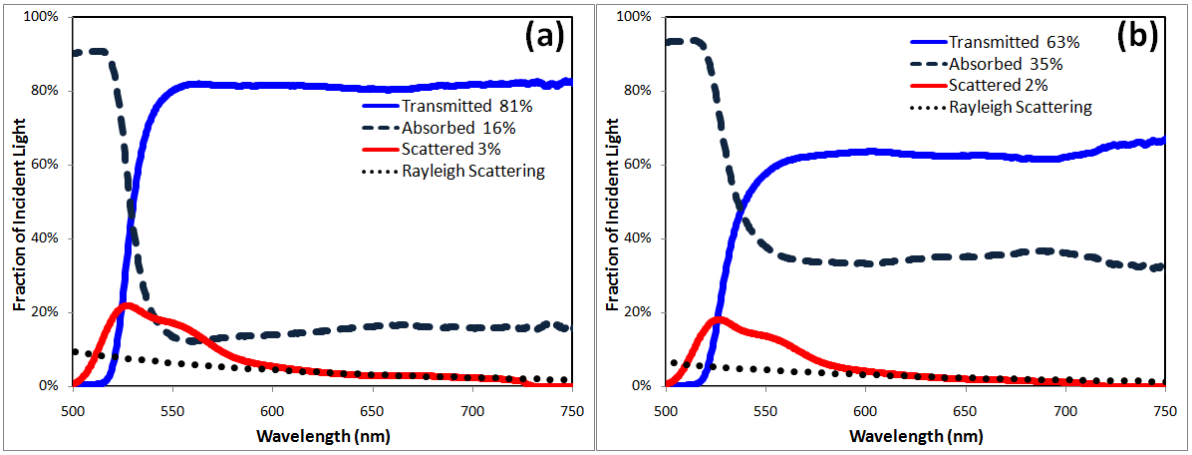

Figure 3 (Color online) Tails extinction measurements for 1.2 m long green LSC Sample 1 (a) before exposure (b) after 6 days outdoor exposure; Transmission (blue), absorption (dashed line), scattering (red) and fitted Rayleigh scattering curve (dotted line).

spectrum has two peaks at 525 nm and 555 nm, which correspond to the characteristic secondary and tertiary emission peaks of the Lumogen F083 dye. Therefore, this portion of the side-scattered spectrum was attributed to dye emission, and was therefore excluded from the energy balance in equations (7) and (8). Hence for this sample, calculations of $\overline{T}$, $\overline{S}$ and $\overline{A}$ have been restricted to the region 600 nm $\leq \lambda \leq$ 750 nm to avoid interference from dye emission. The apparatus could be improved to reduce the emitted component by adding a small piece of the same LSC orthogonal to the light source optic fibre, between the fibre and the LSC. This filter would absorb a large portion of the photons within the absorption region of the dye, significantly reducing unwanted fluorescent emission from the sample.

Table 1 shows the mean tails transmission, absorption and scattering components for the LSC before and after outdoor exposure. Before exposure, the LSC showed high transmission in the tails region ($\overline{T}$ = 81.6 $\pm$ 0.5%), with 2.6 $\pm$ 0.5% extinction due to scattering and 15.8 $\pm$ 0.7% due to absorption. After outdoor exposure, the tails transmission dropped considerably ($\overline{T}$ = 63.5 $\pm$ 0.5%), while the scattering component remained very small ($\overline{S}$ = 1.6 $\pm$ 0.5%). However, the initial mean scattering value of $\overline{S}$ = 2.6 $\pm$ 0.5% would be expected to drop to $\overline{S}$ = 2.0 $\pm$ 0.5% due to the measured reduction

Table 1 – Mean transmission and extinction components in the wavelength range 600 – 750 nm for a green LSC containing *Lumogen F083* fluorescent dye, before and after outdoor exposure

Treatment	Exposure (Mlux.h)	$\overline{T}$	$\overline{S}$	$\overline{A}$
Initial	0	$81.6 \pm 0.5\%$	$2.6 \pm 0.5\%$	$15.8 \pm 0.7\%$
Exposed 6 days	2.43	$63.5 \pm 0.5\%$	$1.6 \pm 0.5\%$	$34.9 \pm 0.7\%$

in LSC transmission. This value is not significantly different from the observed scattering component after exposure, $\overline{S}$ = 1.6 $\pm$ 0.5%. In other words, the scattering component after outdoor exposure was not significantly different from the initial value. Therefore by deduction, the marked decrease in transmission observed for this LSC sample after exposure is due to increased tails absorption (from $\overline{A}$ = 15.8 $\pm$ 0.5% to $\overline{A}$ = 34.9 $\pm$ 0.5%). Hence this LSC sample is highly unstable, as the tails absorption more than doubled after only 6 days outdoors underneath a UV cover.

It is believed that the poor photostability in this LSC is due to photooxidation of dye molecules from interactions with impurities in the matrix during photoexcitation. It is suspected that ketone impurities in the matrix may be responsible. Some of our recently published experimental results confirm that ketones can cause significant photodegradation in *Lumogen F083* dye solutions, and that photostability may be improved by adding an anti-oxidant [11]. However, further work is required to confirm the benefit of using antioxidants in solid PMMA samples. Nonetheless, the data in Figure 3 and Table 1 confirm that the photoproducts formed in this LSC during outdoor exposure are predominantly absorbing in nature, rather than scattering. As shown below, these absorbing photoproducts cause a significant reduction in LSC luminous output, which is accompanied by a relatively small decrease in fluorescent absorption. Further work is required to confirm the cause of the instability and identify potential means of improving photostability in PMMA LSC's.

3.2 Overall Performance

Four performance parameters were measured for the LSC tested above, using different sized LSC samples before exposure and after exposure outdoors underneath a UV cover. All samples were cut from the same master sheet, and exposed simultaneously with the same conditions, so the photodegradation curves are directly comparable. Dye absorption was monitored using 50 mm x 65 mm x 2 mm samples, by measuring the attenuation coefficient α (m^{-1}) over a 2 mm path length, at the dye's peak absorption wavelength of 472 nm. Absorption was measured with a *Cary 5E UV-VIS-NIR* spectrometer. The output luminous flux (*F)*, and half-length ($L_{½}$) were measured using the same sample that was analysed in section 3.1, with dimensions 1200 mm x 150mm x 2 mm. $L_{½}$ is defined as the path length over which 50% of the fluorescently emitted light is lost due to extinction. Half-lengths were measured using the experimental method described in [8]. *F* was measured from one of the small end surfaces using a *Minolta CL-200* lux meter and a 500 mm diameter integrating sphere, by illuminating the sample with two 1.2 m long fluorescent tubes (one UV tube and one 'Daylight' tube). The mean tails transmission ($\overline{T}$) was measured over a 300 mm path length using a 300 mm x 100 mm x 2 mm sample, and the measured attenuation losses were scaled to the same path length as the full-sized LSC (1.2 m), for comparison to $L_{½}$ and *F*. Each parameter was divided by its initial value to give relative performance after exposure, and the degradation curves are plotted in Figure 4.

From Figure 4 it is evident that some fluorescence quenching occurred in this LSC, as the dye absorption dropped by 9% after 14 days exposure. However, the best indicator of LSC performance for lighting applications is the output luminous flux, *F,* which dropped by approximately 50% over the same time period. Hence these measurements confirm the poor photostability of this LSC. Furthermore, $L_{½}$ and $\overline{T}$ are both strongly correlated with the output luminous flux, showing similar reductions of about 50% after 14 days – approximately five times the corresponding reduction

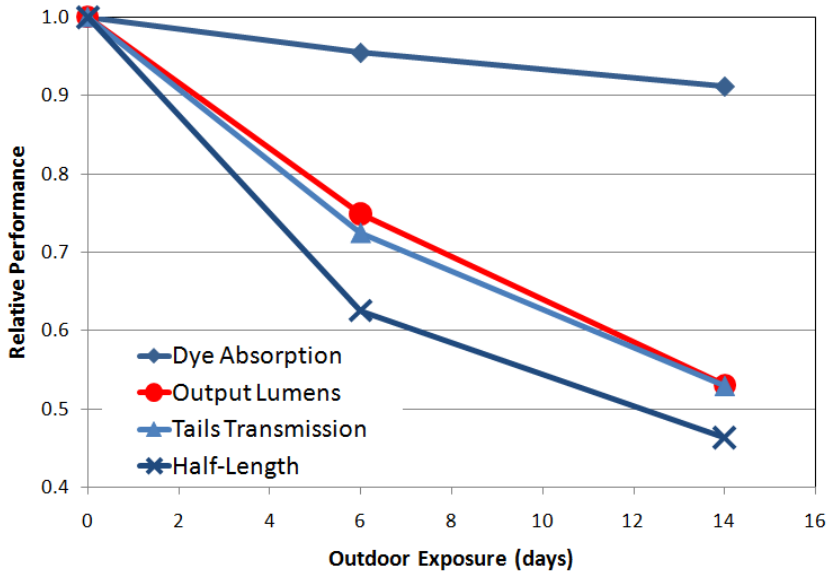

Figure 4 (Color online) Relative performance of green LSC after outdoor exposure; dye absorption (diamonds), output luminous flux (circles), mean tails transmission (triangles) and half-length (crosses)

observed in dye absorption. Hence for large area LSC's, the output luminous flux is around five times more sensitive to changes in tails absorption than it is to fluorescence quenching.

This is an important result with strong implications for the way LSC's are tested for photostability. As indicators of overall LSC performance, *F,* $L_{½}$ and $\overline{T}$ are more informative than dye absorption, as they are each very sensitive to small changes in the light transport properties within the LSC, whereas dye absorption measurements only give information about fluorescence quenching, which does not have a strong effect on LSC luminous output. For photovoltaic applications of LSC's, the wavelength range of interest is not limited to visible light, so the ultimate performance parameter is the power generated by the solar cells, rather than the luminous flux. In this case, the wavelength range for measurement of $L_{½}$ and $\overline{T}$, may be chosen to suit a particular dye or solar cell response. Nonetheless, whatever the wavelength range, $L_{½}$ and $\overline{T}$ are very valuable parameters for describing overall LSC efficiency, particularly for large area LSC's, due to their high sensitivity to tails extinction.

Conclusions

An experimental method is described above for monitoring long wavelength tails extinction in LSC's, and mathematically subdividing the extinction into scattering and absorption components. Measurements on a green PMMA LSC containing *Lumogen F083* dye indicated a sharp rise in tails absorption after only 6 days exposure outdoors underneath a UV cover. However, the scattering component remained fairly constant after exposure, indicating that the main source of extinction losses for this LSC was an absorbing photoproduct.

By comparing the dye absorption, light transport properties and output luminous flux of the same LSC after exposure, it was found that the overall LSC performance was approximately five times more sensitive to tails absorption than to fluorescence quenching. Hence low tails absorption levels are crucial for maintaining high collector output. These results highlight the importance of monitoring tails absorption in LSC's after outdoor exposure, as a sensitive test for the presence of absorbing photoproducts.

Acknowledgements

The authors would like to thank Skydome Holdings Ltd for their financial backing for this work.

References

1. S. T. Bailey, G. E. Lokey, M. S. Hanes, J. D. M. Shearer, J. B. McLafferty, G. T. Beaumont, T. T. Baseler, J. M. Layhue, D. R. Broussard, Y.-Z. Zhang, and B. P. Wittmershaus, "Optimized excitation energy transfer in a three-dye luminescent solar concentrator," Solar Energy Materials and Solar Cells **91,** 67-75 (2007).
2. M. G. El-Shaarawy, S. M. El-Bashir, M. Hammam, and M. K. El-Mansy, "Bent fluorescent solar concentrators (BFSCs): Spectroscopy, stability and outdoor performance," Current Applied Physics **7,** 643-649 (2007).
3. A. M. Hermann, "Luminescent solar concentrators--A review," Solar Energy **29,** 323-329 (1982).

4. A. F. Mansour, "Optical efficiency and optical properties of luminescent solar concentrators," Polymer Testing **17,** 333-343 (1998).
5. R. Reisfeld, D. Shamrakov, and C. Jorgensen, "Photostable solar concentrators based on fluorescent glass films," Solar Energy Materials and Solar Cells **33,** 417-427 (1994).
6. W. G. J. H. M. van Sark, Keith W.J. Barnham, Lenneke H. Slooff, Amanda J. Chatten, A. Büchtemann, A. Meyer, S. J. McCormack, R. Koole, D. J. Farrell, R. Bose, E. E. Bende, A. R. Burgers, T. Budel, J. Quilitz, M. Kennedy, T. Meyer, C. D. M. Donegá, A. Meijerink, and D. Vanmaekelbergh, "Luminescent Solar Concentrators - a Review of Recent Results " Optics Express **16,** 21773 - 21791 (2008).
7. V. Wittwer, W. Stahl, and A. Goetzberger, "Fluorescent planar concentrators," Solar Energy Materials **11,** 187 - 197 (1984).
8. A. A. Earp, G. B. Smith, J. Franklin, and P. Swift, "Optimisation of a three-colour luminescent solar concentrator daylighting system," Solar Energy Materials and Solar Cells **84,** 411-426 (2004).
9. A. F. Mansour, "Outdoor testing of luminescent solar concentrators in a liquid polymer and bulk plate of PMMA," Polymer Testing **17,** 153-162 (1998).
10. A. V. Deshpande, and E. B. Namdas, "Correlation between lasing and photophysical performance of dyes in polymethylmethacrylate," Journal of Luminescence **91,** 25-31 (2000).
11. A. A. Earp, T. Rawling, J. Franklin, and G. B. Smith, "Perylene Dye Degradation due to Ketones and singlet oxygen," Dyes and Pigments**,** (2009).
12. G. Seybold, and G. Wagenblast, "New perylene and violanthrone dyestuffs for fluorescent collectors," Dyes and Pigments **11,** 303-317 (1989).
13. A. A. Earp, G. B. Smith, P. D. Swift, and J. Franklin, "Maximising the light output of a Luminescent Solar Concentrator," Solar Energy **76,** 655-667 (2004).
14. W. R. L. Thomas, J. M. Drake, and M. L. Lesiecki, "Light transport in planar luminescent solar concentrators: the role of matrix losses," Applied Optics **22,** 3440 - 3450 (1983).